AD-A245 641

AD

TECHNICAL REPORT ARCCB-TR-91035

CRACK ARREST AND STATIC FRACTURE TOUGHNESS TESTS OF A SHIP PLATE STEEL

J. H. UNDERWOOD
I. A. BURCH
J. C. RITTER

DECEMBER 1991

US ARMY ARMAMENT RESEARCH, DEVELOPMENT AND ENGINEERING CENTER
CLOSE COMBAT ARMAMENTS CENTER
BENÉT LABORATORIES
WATERVLIET, N.Y. 12189-4050

DISCLAIMER

The findings in this report are not to be construed as an official Department of the Army position unless so designated by other authorized documents.

The use of trade name(s) and/or manufacturer(s) does not constitute an official indorsement or approval.

DESTRUCTION NOTICE

For classified documents, follow the procedures in DoD 5200.22-M, Industrial Security Manual, Section II-19 or DoD 5200.1-R, Information Security Program Regulation, Chapter IX.

For unclassified, limited documents, destroy by any method that will prevent disclosure of contents or reconstruction of the document.

For unclassified, unlimited documents, destroy when the report is no longer needed. Do not return it to the originator.

REPORT DOCUMENTATION PAGE

Form Approved
OMB No 0704-0188

1. AGENCY USE ONLY *(Leave blank)*	2. REPORT DATE	3. REPORT TYPE AND DATES COVERED
	December 1991	Final

4. TITLE AND SUBTITLE
CRACK ARREST AND STATIC FRACTURE TOUGHNESS TESTS OF A SHIP PLATE STEEL

5. FUNDING NUMBERS
AMCMS: 6111.02.H610.011
PRON: 1A05Z0CANMSC

6. AUTHOR(S)
J.H. Underwood, I.A. Burch* and J.C. Ritter*
*Materials Research Laboratory, Defence Science & Technology Organisation, Melbourne, Australia

7. PERFORMING ORGANIZATION NAME(S) AND ADDRESS(ES)
U.S. Army ARDEC
Benet Laboratories, SMCAR-CCB-TL
Watervliet, NY 12189-4050

8. PERFORMING ORGANIZATION REPORT NUMBER
ARCCB-TR-91035

9. SPONSORING/MONITORING AGENCY NAME(S) AND ADDRESS(ES)
U.S. Army ARDEC
Close Combat Armaments Center
Picatinny Arsenal, NJ 07806-5000

10. SPONSORING/MONITORING AGENCY REPORT NUMBER

11. SUPPLEMENTARY NOTES
Presented at ASTM Symposium on Rapid Load Fracture Testing, San Francisco, CA, April 1990.
Published in ASTM STP.

12a. DISTRIBUTION/AVAILABILITY STATEMENT
Approved for public release; distribution unlimited.

12b. DISTRIBUTION CODE

13. ABSTRACT *(Maximum 200 words)*
The recently standardized ASTM crack arrest fracture toughness test method was modified for use with an Australian low alloy, 700 MPa strength, quenched and tempered steel used for ship plate. Specimens 50-mm thick in longitudinal and transverse orientations were tested at -60°C with various depths of side groove. Specimen configurations somewhat outside the range of the ASTM method were found to be useful for this steel and were suggested as modifications to the standard method. A different solution and expression for the stress intensity factor was used to evaluate the tests and to develop a method for predicting the crack length at which a running crack will arrest. Good agreement was obtained between the observed and predicted crack lengths at arrest. The wedge-loading arrangement of the crack arrest test procedure was used for static fracture toughness tests. Procedures for static wedge-loading fracture toughness were proposed for use, particularly for comparisons with crack arrest toughness test results obtained under similar test conditions. The static fracture toughness was more than twice the value of crack arrest toughness for the tests in this report.

14. SUBJECT TERMS
Crack Arrest, Fracture Toughness, Ship Plate, K Expression

15. NUMBER OF PAGES
26

16. PRICE CODE

17. SECURITY CLASSIFICATION OF REPORT	18. SECURITY CLASSIFICATION OF THIS PAGE	19. SECURITY CLASSIFICATION OF ABSTRACT	20. LIMITATION OF ABSTRACT
UNCLASSIFIED	UNCLASSIFIED	UNCLASSIFIED	UL

TABLE OF CONTENTS

	Page
ACKNOWLEDGMENTS	iii
INTRODUCTION AND OBJECTIVES	1
MATERIAL AND TEST PROCEDURES	2
Material	2
K_{Ia} Tests	4
Wedge-Loaded K_{Ic} Tests	5
RESULTS AND DISCUSSION	6
K_{Ia} and K_{Ic} Results	6
Comparison With Other Results	9
Prediction of Crack Depth at Arrest	11
SUMMARY	13
REFERENCES	16

TABLES

I.	MATERIAL COMPOSITION AND MECHANICAL PROPERTIES	3
II.	CRACK ARREST FRACTURE TOUGHNESS TEST CONDITIONS	7
III.	FRACTURE TOUGHNESS FROM STATIC WEDGE-LOADED TESTS AT -60°C	8
IV.	CRACK ARREST FRACTURE TOUGHNESS RESULTS OF RIPLING AND CROSLEY FOR TWO STEELS TESTED AT -54°C	10
V.	CALCULATED CRACK DEPTH AT ARREST, $(a/W)_a$, FOR VARIOUS VALUES OF $(a/W)_o$, K_{Ia}/K_o, B_N/B, and δ_a/δ_o = 1.10	13

LIST OF ILLUSTRATIONS

1.	Applied J versus crack growth for BIS 690 at +20°C	17
2.	Specimen configuration for K_{Ia} tests	18
3.	Comparison of K/δ results for wedge-loaded compact specimen	19

Page

4. Wedge load versus crack-mouth displacement for K_{Ia} tests of BIS 690 at -60°C 20

5. Photographs of fracture surfaces of K_{Ia} and K_{Ic} specimens 21

6. K_o, K_{Ic}, and K_{Ia} versus notch or crack depth 22

7. Calculated and measured values of $KW^{\frac{1}{2}}/\delta E$ versus crack depth 23

ACKNOWLEDGMENTS

The authors are pleased to acknowledge M.Z. Shah Khan and N.J. Baldwin of the Materials Research Laboratory for their help in fracture and mechanical testing and in developing wedge-loading test procedures, respectively.

INTRODUCTION AND OBJECTIVES

Fracture toughness for rapid load conditions is a common concern with military structures. A long-standing procedure for addressing this concern in ship structures is the explosion bulge test developed by the U.S. Navy (ref 1). This procedure gives an effective simulation of explosive loading conditions of ship plate and has very successfully predicted service behavior. For armament components such as cannons, full-scale fatigue tests using rapid load firing tests have been shown by the U.S. Army to give excellent predictions of service behavior (ref 2). Regardless of how well such full-scale tests can predict service behavior for these components, there are significant drawbacks. Full-scale tests are always time-consuming and expensive, and the test results often can not be directly related to accepted fracture mechanics properties and analysis, thus requiring additional tests when conditions change.

The recently standardized ASTM E-1221 "Standard Test Method For Determining Plane-Strain Crack Arrest Fracture Toughness, K_{Ia}, of Ferritic Steels," may provide a means to directly and quantitatively relate the rapid load fracture behavior of components such as ship plate and cannon to a material fracture property. The advantages of the K_{Ia} method are that it is a reasonably small laboratory test and the results can be directly related to the level of applied stress intensity factor of a loaded component. Therefore, the K_{Ia} test can be used in the same general way that plane-strain fracture toughness, K_{Ic}, is used, i.e., as a critical material property used with fracture mechanics analysis to predict the load and geometry conditions at which fracture will occur.

The overall objective of this work was to demonstrate that K_{Ia} gives a consistent laboratory measure of the crack arrest fracture toughness property of a ship plate steel for various test configurations. The starting notch length and depth of side grooves were chosen as configurational variables in tests with

specimens half the depth, W, of that recommended in ASTM Method E-1221. If consistent results could be obtained with smaller specimens, the test would become a more practical laboratory procedure. The smaller specimen would allow more test location choices, such as around welds in ship plate or at different locations and orientations in cannon components. Rosenfield and co-workers (ref 3) showed that miniature specimens for reactor surveillance testing gave slightly lower K_{Ia} compared with larger specimens from an ASTM A508 steel.

As the investigation proceeded, some progress was noted in the test configurations used outside the recommended range and the analysis used to predict conditions for a successful arrest of a running crack. Therefore, a second objective of the investigation became the development of modified K_{Ia} test and analysis procedures for this steel and their proposed use for K_{Ia} testing in general.

MATERIAL AND TEST PROCEDURES

Material

The steel used for the tests was Australian BIS 690, a 50-mm thick, low alloy ship plate steel, quenched and tempered to a nominal 700 MPa strength. The chemical composition and mechanical properties of the plate from which all specimens were taken are given in Table I. The initial plan was to perform the K_{Ia} tests at -40°C, a typical low service temperature for military hardware. Note that the Charpy energy in Table I at -40°C is considerably above the general recommendation of 41 J for a successful K_{Ia} test (ref 3). This recommendation proved to be good advice; all but one test were performed at a lower temperature, -60°C, in order to obtain successful crack arrests.

TABLE I. MATERIAL COMPOSITION AND MECHANICAL PROPERTIES

Composition	Weight Percent
Copper	0.16
Manganese	1.5
Silicon	0.40
Nickel	0.25
Chromium	0.35
Molybdenum	0.40
Boron	0.005
Titanium	0.05
Niobium	0.05
Vanadium	0.09

Mechanical Properties						
Yield Strength L, +20°C MPa	Tensile Strength L, +20°C MPa	Fracture Toughness From J_{Ic} Tests T-L, +20°C MPa $m^{1/2}$	Charpy Energy Joules, T-L Temperature °C			
			0	-20	-40	-50
701	762	239	91	87	78	60

The room temperature fracture toughness of the material was characterized by J_{Ic} tests of 25-mm thick compact specimens, which yielded a mean J_{Ic} value of 251 KN/m and corresponding K value of 239 MPa $m^{1/2}$. One of the two J versus Δa plots is shown as Figure 1. Unloading compliance was used to determine Δa, following ASTM E-813, "Standard Test Method for J_{Ic}, A Measure of Fracture Toughness," with one addition. A single point at a J value of about two-thirds of the expected J_{Ic} was used as a reference point. Shifting this point (and all data) to fall exactly on the blunting line involved the use of an effective

elastic modulus, E, of 209.7 GPa, compared with the initial nominal value of 210.0 GPa. For the tests in this report, the reference point technique effectively addressed Δa shifts of the data, a common problem in J_{Ic} tests.

K_{Ia} Tests

The crack arrest test specimens shown in Figure 2 followed the recommendations of ASTM E-1221 except for two modifications. First, the side groove depth was varied from $B_N/B = 0.75$ (recommended) to $B_N/B = 1$. Second, the initial notch was varied from $a_o/W = 0.30$ (the minimum recommended) to $a_o/W = 0.16$. The width-to-thickness ratio, W/B, was 2.0, which, although not outside the recommended range, $2.0 \leq W/B \leq 8.0$, was half the value commonly used. For a given plate thickness, a specimen with W/B = 2 is less likely to result in arrest than a specimen with a larger face dimension. However, since the W/B = 2 specimen is more useful, as discussed earlier, it is worth pursuing.

A brittle weld was added at the notch tip (using Hardex N electrodes), and the wedge load-type tests of T-L and L-T orientations were performed generally at -60°C. The low temperature was attained by pumping a liquid and gas mixture of nitrogen into a foam plastic enclosure around the specimen. The side groove, the initial notch conditions, the initial displacement, δ_o, and the resulting initial applied stress intensity, K_o, for the tests are listed in Table II. The following expression, although different from that in ASTM E-1221, is used to calculate the ratio K/δ as a function of a/W (ref 4):

$$KW^{1/2}/\delta E[1-a/W]^{1/2} = 0.748 - 2.176(a/W) + 3.56(a/W)^2 - 2.55(a/W)^3 + 0.62(a/W)^4 \quad \text{for } 0.2 \leq a/W \leq 1.0 \qquad (1)$$

This expression gives results similar to that in ASTM E-1221 for $0.4 \leq a/W \leq 0.6$, but differs elsewhere. For a/W = 0.8, a crack length often used in K_{Ia} tests, Eq. (1) gives a value 7 percent higher than the E-1221 expression. The

E-1221 expression is repeated below for reference purposes:

$$KW^{1/2}/\delta E = \frac{2.24\ [1.72 - 0.9(a/W) + (a/W)^2]\ [1-a/W]^{1/2}}{[9.85 - 0.17(a/W) + 11(a/W)^2]}$$

$$\text{for } 0.30 \leq a/W \leq 0.85 \qquad (2)$$

A comparison of the K/δ expression from collocation analysis (ref 4), Eq. (1), with that from ASTM E-1221 based on experimental compliance tests, Eq. (2), is shown in Figure 3. Pajot's recent finite element results for the same wedge-loaded compact configuration (ref 5) are also shown. The two independent sets of analytical results agree within 2 percent for a/W up to 0.5 and within 1 percent for $0.5 \leq a/W \leq 0.95$. Both sets of analytical results agree well, within 2 percent, with the experimental results for a/W up to 0.6, as noted earlier. For deeper cracks, the two types of K/δ results diverge. Considering that independent analyses agree well for all crack lengths, and experimental methods can be subject to unavoidable errors for deep cracks (ref 4), the Eq. (1) relation from analysis was used for the tests here.

Wedge-Loaded K_{Ic} Tests

Static load fracture toughness tests were performed at -60°C in T-L and L-T orientations using the configuration shown in Figure 2 with minor modifications. Holes 15-mm in diameter were added for pin loading in fatigue to precrack the samples. Wedge load was applied quasi-statically until failure, as in a standard K_{Ic} test. Because of the inherent high stiffness of the wedge load arrangement, the load-displacement trace changed quite abruptly as crack growth began; the trace showed a sharp drop in a manner very similar to the K_{Ia} test of specimen #6 in Figure 4. This resulted in an unambiguous determination of the critical K value for initiation of crack growth. Equation (1) and the same general procedures used for K_{Ia} determination were used to determine K_{Ic}. For these

tests. the wedge load compact specimen arrangement was quite suitable to measure static plane-strain fracture toughness.

RESULTS AND DISCUSSION

K_{Ia} and K_{Ic} Results

Tabular results of the K_{Ia} and K_{Ic} tests are listed in Tables II and III. The final notch lengths marked by heat tinting and the related values of crack arrest fracture toughness are shown in Table II. Note that for the tests with $B_N/B = 0.75$ and a_o/W of 0.3 or more, only one test, that with the smallest a_o/W and δ_o, resulted in a proper arrest. Since a_o/W could be directly controlled, it was intentionally varied in subsequent tests, along with the planned variation in B_N/B. As expected, both higher B_N/B and lower a_o/W favored arrest, although a small change in a_o/W had a surprisingly large effect on arrest. This observation prompted a predictive analysis, described in an upcoming section.

Plots of wedge load versus crack-mouth displacement, δ, for two K_{Ia} tests are shown in Figure 4. Specimen #6 had B_N/B and a_o/W as recommended by ASTM E-1221; specimen #19 had a configuration outside the recommendations. As expected, specimen #19 was much stiffer, but the general behavior and the resulting K_{Ia} (in Table II) were quite similar. The overall K_{Ia} results, indicated by the individual and mean values in Table II, show a relatively consistent crack arrest toughness with no readily apparent effects of material orientation, depth of side grooves, depth of initial notch, and initial applied K. It is believed that using a much shallower initial notch rather than that recommended in ASTM E-1221 did not affect the K_{Ia} results because of the significant amount of crack growth that occurred beyond the initial notch.

TABLE II. CRACK ARREST FRACTURE TOUGHNESS TEST CONDITIONS

Specimen #/ Orientation/ Temperature	Side Groove B_N/B	Initial Conditions			Arrest Conditions		
		Notch: $(a/W)_o$	δ: δ_o mm	K: K_o MPa $m^{1/2}$	Notch: $(a/W)_a$	δ: δ_a mm	K: K_{Ia} MPa $m^{1/2}$
At -40°C:							
5 T-L	0.76	0.34	0.97	197	1.00	--	--
At -60°C:							
4 T-L	0.76	0.35	0.75	149	1.00	--	--
1 L-T	0.76	0.35	0.75	149	0.96	--	--
2 L-T	0.76	0.44	0.91	148	0.97	--	--
6 L-T	0.76	0.30	0.52	116	0.78	0.57	48
3 T-L	0.88	0.31	0.58	117	0.76	0.63	52
8 T-L	0.88	0.18	0.48	141	0.79	0.56	43
9 T-L	0.88	0.18	0.52	151	0.65	0.58	60
14 L-T	0.88	0.35	0.61	113	0.80	0.64	47
16 L-T	0.88	0.32	0.47	94	0.64	0.51	54
17 T-L	1.00	0.19	0.37	99	0.45	0.41	57
19 T-L	1.00	0.18	0.34	93	0.42	0.37	55
7 L-T	1.00	0.16	0.38	112	0.41	0.41	62
18 L-T	1.00	0.18	0.31	86	0.47	0.37	49

L-T mean K_{Ia}:	52.0 MPa $m^{1/2}$	6.2 standard deviation
T-L mean K_{Ia}:	53.4	6.5
grand mean K_{Ia}:	52.7	6.0

The results of the static wedge load fracture toughness tests are given in Table III. Note that the results were not valid by the usual specimen thickness, B, criterion. A -60°C yield strength, σ_{-60}, of 757 MPa was used, which is 8 percent above the +20°C value from Table I, based on results from the

literature (ref 6) for a similar steel. Even with this higher yield strength, the thickness criterion was not met. However, this is offset to some extent by the abrupt drop of load as crack growth began, as noted earlier. The results of the static fracture toughness tests can be related to some features of the K_{Ia} tests. Note that the highest values of K_o in the -60°C K_{Ia} tests, about 150 MPa $m^{1/2}$, are about equal to the static toughness values. This is probably an indication that, for those tests, the crack grew through the brittle weld, stopped, and later reinitiated in the parent plate at $K \approx K_{Ic}$, to begin the run arrest event. Some of the test traces showed a pop-in well before the point at which the crack ran, interpreted as a pop-in in the weld, which supports the above supposition.

TABLE III. FRACTURE TOUGHNESS FROM STATIC WEDGE-LOADED TESTS AT -60°C

Specimen	Orientation	Fracture Toughness MPa $m^{1/2}$	$[2.5(K_{Ic}/\sigma_{-60})^2]/B$
a	L-T	147	1.88
b	L-T	111	1.08
c	T-L	142	1.76
d	T-L	156	2.12
grand mean 139 MPa $m^{1/2}$ standard deviation 19.5			

Photographs of fracture surfaces of three K_{Ia} specimens and one K_{Ic} specimen are shown in Figure 5. Skewed crack growth was seen with four of the ten successful K_{Ia} tests. Specimen #6 was the worst observed; the slight degree of skew shown for specimen #18 was typical. We believe the skewed crack growth was due to misalignment of the loading hole or the specimen support on individual K_{Ia} specimens, because it occurred sporadically for K_{Ia} tests and not at all for static tests.

A graphical summary of all the static and crack arrest fracture toughness results is given in Figure 6. The values of K_o at the start of run arrest, the K_{Ia} values, and the static test data are plotted versus their respective crack depths, a/W. The correspondence between the higher values of K_o and the static fracture toughness data noted earlier can be seen. Regression analysis was performed to check for significant quantitative effects of test variables on K_{Ia}, including $(a/W)_a$, $(a/W)_o$, B_N/B, and K_o. Of these variables, only $(a/W)_a$ showed a correlation coefficient larger (in absolute value) than 0.5; its value was -0.66. Therefore, there was some decrease in K_{Ia} with increasing final crack depth (indicated by the solid line) from regression analysis. This decrease in K_{Ia} could also be attributed to an increasing amount of crack jump, since crack jump is not independent of final crack depth in these tests. These effects and explanations for a decrease in K_{Ia} have been noted before (ref 3). It is emphasized that had the K/δ relation from E-1221 been used to analyze these K_{Ia} results, the effect of decreasing K_{Ia} for deep cracks would have been more apparent. To demonstrate this point, the ten K_{Ia} results were recalculated using the E-1221 relation (Eq. (2)); the dashed line, a regression fit to these results, is shown in Figure 6, and an additional decrease of K_{Ia} with a/W can be seen.

Comparison With Other Results

It is interesting to compare the K_{Ia} results here with those from other similar tests. Ripling and Crosley (ref 6) tested AISI 1340 and 4140 steels at -54°C, a reasonably appropriate comparison to this work, although the yield strengths were somewhat higher in their work. Table IV summarizes some of their results. The results for 1340 steel, probably the more appropriate comparison, are in good agreement with the results here. Their 4140 steel results also agree well with the results here, except for the lowest strength material.

This could be explained by the significant transition with temperature which Ripling and Crosley noted in their K_{Ia} results.

TABLE IV. CRACK ARREST FRACTURE TOUGHNESS RESULTS OF RIPLING AND CROSLEY FOR TWO STEELS TESTED AT -54°C

AISI 1340 Steel		AISI 4140 Steel	
σ_Y, +20°C MPa	K_{Ia} MPa $m^{1/2}$	σ_Y, +20°C MPa	K_{Ia} MPa $m^{1/2}$
965	70	965	154
1100	51	1100	60
1240	50	1240	51

An important difference between the overall results of this investigation and results of other types of rapid load fracture tests can be emphasized by comparison with results of dynamic initiation fracture toughness tests. Kendall (ref 7) was among the first to investigate dynamic K_{Ic} in high strength steels. He found no effect of loading rate in valid-sized K_{Ic} results for AISI 4340 steel of 1275 MPa yield strength tested at -51°C with a K rate of 105 MPa $m^{1/2}$/sec. Some recent work (ref 8) compared static K_{Ic} with dynamic initiation K values determined from nonstandard J_{Ic} tests of 4340 vacuum-arc-remelt steel. They found typically twofold increases in dynamic initiation toughness compared to static when tested at K rates of 2 x 106 MPa $m^{1/2}$/sec over a wide range of temperature from -140° to +100°C. It is important to note that dynamic initiation toughness, K_{Id}, has been found (refs 7,8) to be equal to or greater than K_{Ic} for this type of steel, whereas K_{Ia} is significantly less than K_{Ic} in the tests here. This significant difference may be caused by the clear difference in fracture process, initiation of crack growth under rapid load in one case, and rapid run arrest growth in the other.

Prediction of Crack Depth at Arrest

The significant decrease in the crack depth at arrest brought about by a small decrease in initial crack depth in these tests led to the following method of predicting the crack depth at arrest.

First, an expression for a/W in terms of the K parameter for the wedge load compact, $KW^{1/2}/\delta E$, is required. This expression, essentially the inverse of Eq. (1), was developed here by regression analysis of data from Eq. (1) and is given as follows:

$$a/W = f(V) = 1 + 1.132\ V - 47.29\ V^2 + 206.3\ V^3 - 359.2\ V^4 + 225.5\ V^5$$
$$\text{where } V = KW^{1/2}/\delta E \quad ; \quad \text{for } 0.15 \leq a/W \leq 1.00 \tag{3}$$

Equation (3) is compatible with Eq. (1) within 0.02 W over the indicated range of a/W and within 0.007 W over the range $0.15 \leq a/W \leq 0.85$.

Using the expression of Eq. (3), a prediction of crack depth at arrest, $(a/W)_a$, can be made as follows:

$$(a/W)_a = f(V_a) \quad ; \quad V_a = K_{Ia}(B_N/B)^{1/2}W^{1/2}/(\delta_a/\delta_o)\delta_o E \tag{4}$$

where the function, f, is from Eq. (3). The effect of side grooving is accounted for by the $(B_N/B)^{1/2}$ term. Side grooves lower the specimen's ability to arrest a crack, and this can be represented by an effective K_{Ia} equal to K_{Ia} x $(BN/B)^{1/2}$. The combination $(\delta_a/\delta_o)\delta_o$ represents the crack-mouth displacement at arrest, δ_a, obtained by using the experimental observation that δ_a is generally a bit larger than δ_o by a constant ratio. For the tests here, the mean value of δ_a/δ_o was 1.10, as seen in Table II.

The after-the-fact predictions of $(a/W)_a$ were made using Eq. (4) to check the procedure. The results, shown in Figure 7 for all thirteen tests at -60°C, include the three in which the crack depth at arrest was beyond the a/W = 0.85 limit of ASTM E-1221. The open symbols are the values of V_a = $[K_{Ia-ave}(B_N/B)^{1/2}W^{1/2}/1.1\ \delta_o E]$ plotted versus measured $(a/W)_a$, where K_{Ia-ave} is

52.7 MPa $m^{1/2}$ from Table II; $(a/W)_a$, B_N/B, and δ_o are from Table II; and W and E are 0.100 m and 210 GPa, respectively. The predicted values, shown as an X, are the same values of V_a plotted versus the values of a/W calculated from Eq. (3). The predicted values of a/W are in good agreement with the measured values for all but the deepest cracks. This is significant because it indicates that the important effects of initial notch depth and side groove depth can be included in a mechanics-based prediction of the crack depth at arrest before a K_{Ia} test is performed. However, since a measured value of δ_a/δ_o was used, this prediction has its limitations.

Another, more general type of prediction of crack depth at arrest can be made using the procedure outlined by Eq. (4). By assuming various values of the ratio of K_{Ia} for the material of interest to the applied K at initiation of the run arrest event, K_o, calculations of crack depth at arrest can be made for various prescribed combinations of $(a/W)_o$, B_N/B, and δ_a/δ_o. Table V lists such calculations for the value of δ_a/δ_o from these tests, 1.10, and two values of B_N/B. For tests in which the run arrest begins from a crack in the parent material rather than at a brittle weld, $K_o \approx K_{Ic}$. As noted earlier, this was the situation for some of the tests here. For $K_o \approx K_{Ic}$, Table V can be used to make general predictions of arrest behavior for a given combination of material and test configuration. For example, for a material with K_{Ia} nearly equal to K_{Ic}, arrest is easy to manage even for a relatively deep initial notch and side grooves, as indicated by the first few columns in Table V. For a material with K_{Ia}, which is half or less of K_{Ic}, arrest is likely only for a relatively shallow initial notch and shallow or nonexistent side grooves, which were generally the configurations of the successful tests here.

TABLE V. CALCULATED CRACK DEPTH AT ARREST, $(a/W)_a$, FOR VARIOUS VALUES OF $(a/W)_o$, K_{Ia}/K_o, B_N/B, and $\delta_a/\delta_o = 1.10$

	$K_{Ia}/K_o = 0.8$	0.7	0.6	0.5	0.4	0.3
$B_N/B = 1.00$						
$(a/W)_o$ = 0.2:	0.31	0.37	0.44	0.54	0.67	0.80
0.3:	0.44	0.51	0.60	0.70	0.79	0.87
0.4:	0.57	0.65	0.72	0.80	0.86	0.92
0.5:	0.68	0.74	0.80	0.85	0.90	0.94
0.6:	0.76	0.81	0.85	0.89	0.93	0.96
$B_N/B = 0.76$						
$(a/W)_o$ = 0.2:	0.37	0.44	0.52	0.63	0.74	0.84
0.3:	0.52	0.60	0.68	0.76	0.84	0.90
0.4:	0.65	0.72	0.78	0.84	0.89	0.94
0.5:	0.75	0.80	0.84	0.89	0.92	0.95
0.6:	0.81	0.85	0.89	0.92	0.94	0.97

SUMMARY

The material characterization results of the investigation can be summarized as follows:

1. The grand mean crack arrest fracture toughness, K_{Ia}, of ten tests of BIS 690 ship plate steel at -60°C was 52.7 MPa $m^{1/2}$, with a standard deviation of 6.0 MPa $m^{1/2}$. Individual mean values for T-L and L-T orientations were within about 1 percent of the grand mean, which shows no significant variation of K_{Ia} with orientation. The K_{Ia} results showed no apparent effect of depth of side grooves or of initial notch. The results did indicate a slight decrease in K_{Ia} with increasing depth of crack at arrest. Regression analysis of the ten test results shows a decrease in K_{Ia} from 57..7 to 49.5 MPa $m^{1/2}$ corresponding to an increase in $(a/W)_a$ from 0.41 to 0.79.

2. The mean static fracture toughness of BIS 690 steel at -60°C determined from wedge-loaded tests similar in procedure and analysis to K_{Ia} tests was 139 MPa $m^{1/2}$. The test specimen thickness was equal to the full 50-mm thickness of the plate, but it did not meet the $2.5(K_{Ic}/\sigma_Y)^2$ validity requirement for a K_{Ic} test of this material at -60°C, calculated as 84 mm.

3. The static fracture toughness of BIS 690 steel at +20°C determined from J_{Ic} tests was 239 MPa $m^{1/2}$.

4. The K_{Ia} of BIS 690 at -60°C was a relatively small fraction of K_{Ic}; K_{Ia}/K_{Ic} = 0.38. This has implications for design and service life analysis of BIS 690 structural components subjected to low temperature. If service conditions allow a crack to run, an initiation fracture toughness approach to design and life analysis would be insufficient at best, possibly nonconservative.

The test method development results of the investigation are the following:

1. Crack arrest tests with somewhat shallower initial notch depths than those recommended in ASTM E-1221, i.e., in the range $0.15 \leq (a/W)_o \leq 0.30$, arrested at significantly shallower crack depths.

2. An expression for crack depth, a/W, in terms of $KW^{1/2}/\delta E$ and an associated analysis for predicting crack depth at arrest gave a good description of the BIS 690 test results at -60°C, including effects of side groove depth and initial notch depth on crack depth at arrest.

3. A static fracture toughness test procedure based on the wedge load arrangement and analysis methods of ASTM E-1221 was suitable for K_{Ic} tests of BIS 690 at -60°C. Aside from the common and unavoidable specimen thickness problems with this relatively tough material, the wedge-loaded K_{Ic} tests were consistent and easily interpreted.

4. Shallower initial notches and the expression and analysis for predicting crack depth at arrest are suggested as future additions to the ASTM E-1221 method for K_{Ia} tests. They address a persistent problem with the method: controlling and predicting the crack depth at arrest.

REFERENCES

1. C.E. Hartbower and W.S. Pellini, "Explosion Bulge Test Studies of the Deformation of Weldments," Welding Journal Research Supplement, Vol. 30, 1951, pp. 307s-318s.
2. T.E. Davidson, J.F. Throop, and J.H. Underwood, "Failure of a 175-mm Cannon and the Resolution of the Problem Using an Autofrettaged Design," Case Studies in Fracture Mechanics, (Thomas P. Rich and David J. Cartwright, eds.), AMMRC MS 77-5, Army Materials and Mechanics Research Center, Watertown, MA, 1977.
3. A.R. Rosenfield, P.N. Mincer, C.W. Marschall, and A.J. Markworth, "Recent Advances in Crack-Arrest Technology," Fracture Mechanics: Fifteenth Symposium, ASTM STP 833, (R.J. Sanford, ed.), American Society for Testing and Materials, Philadelphia, PA, 1984, pp. 149-164.
4. J.H. Underwood and J.C. Newman, Jr., "Comparison of Compliance Results for the Wedge-Loaded Compact Specimen," J. of Testing and Evaluation, Vol. 16, No. 5, September 1988, pp. 489-491.
5. J.J. Pajot, General Electric Company, Schenectady, NY, to be published.
6. E.J. Ripling and P.B. Crosley, "Crack Arrest Toughness of 4140, 1340, 4340 Steel," MRL Report No. 792, Materials Research Laboratory, Inc., Glenwood, IL, November 1981.
7. D.P. Kendall, "The Effect of Loading Rate and Temperature on the Fracture Toughness of High Strength Steels," Materials Research and Standards, Vol. 10, No. 12, December 1970.
8. Y.C. Chi, S.H. Lee, K. Cho, and J. Duffy, "The Effects of Tempering and Test Temperature on the Dynamic Fracture Initiation Behavior of an AISI 4340 VAR Steel," Report #2, Army Contract No. DAAL03-88-K-0015, Brown University, Providence, RI, August 1988.

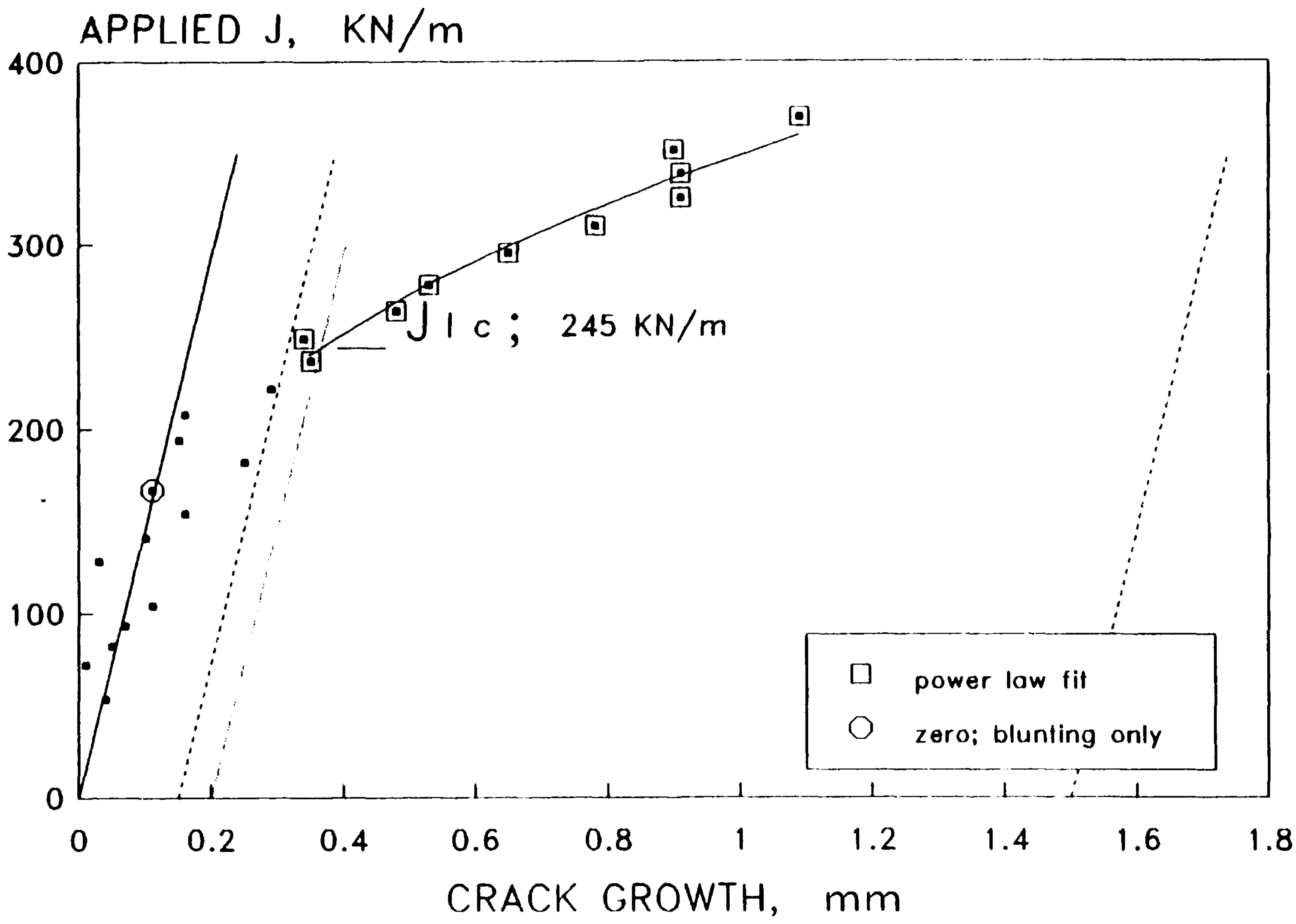

Figure 1. Applied J versus crack growth for BIS 690 at +20°C.

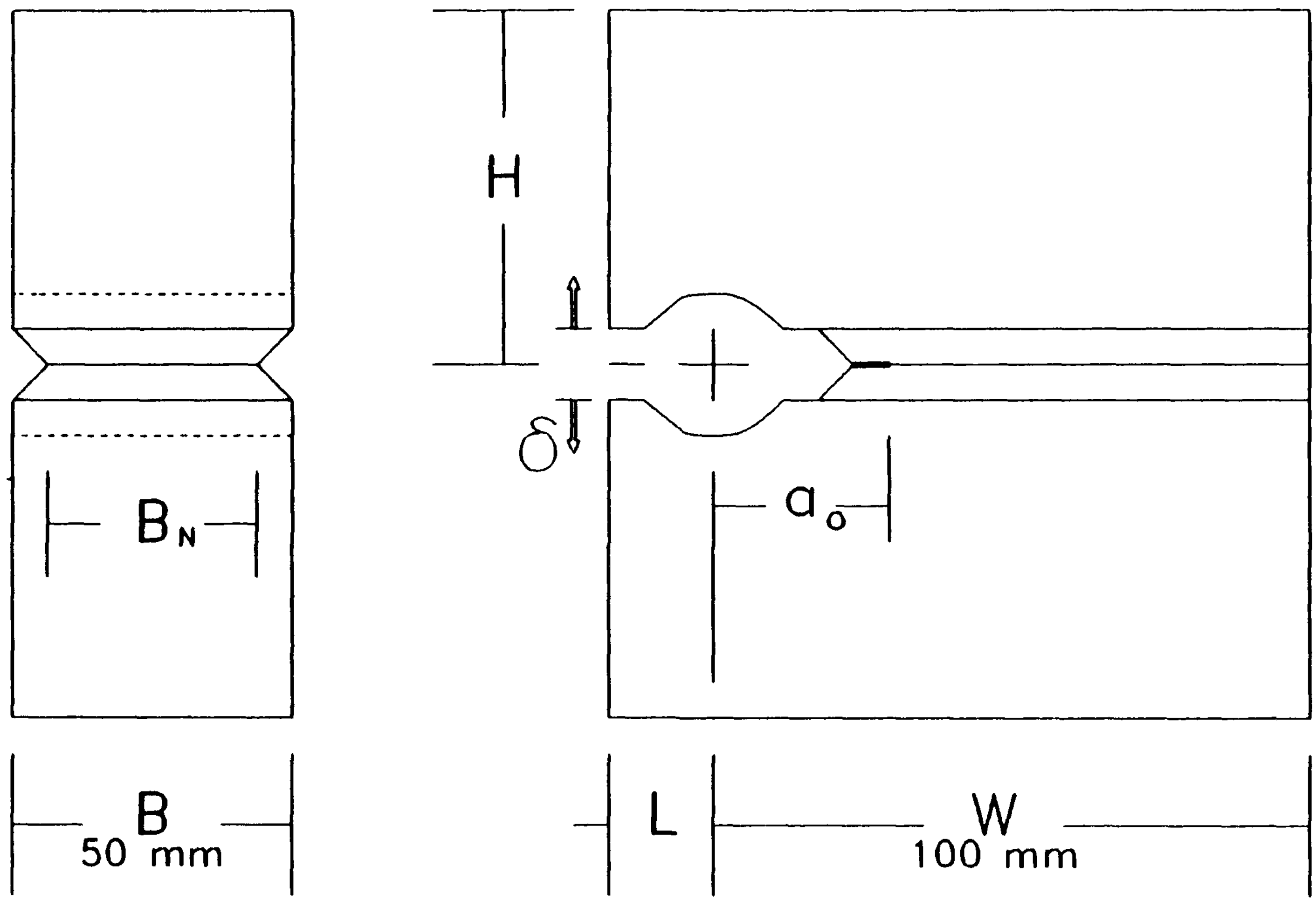

Figure 2. Specimen configuration for K_{Ia} tests.

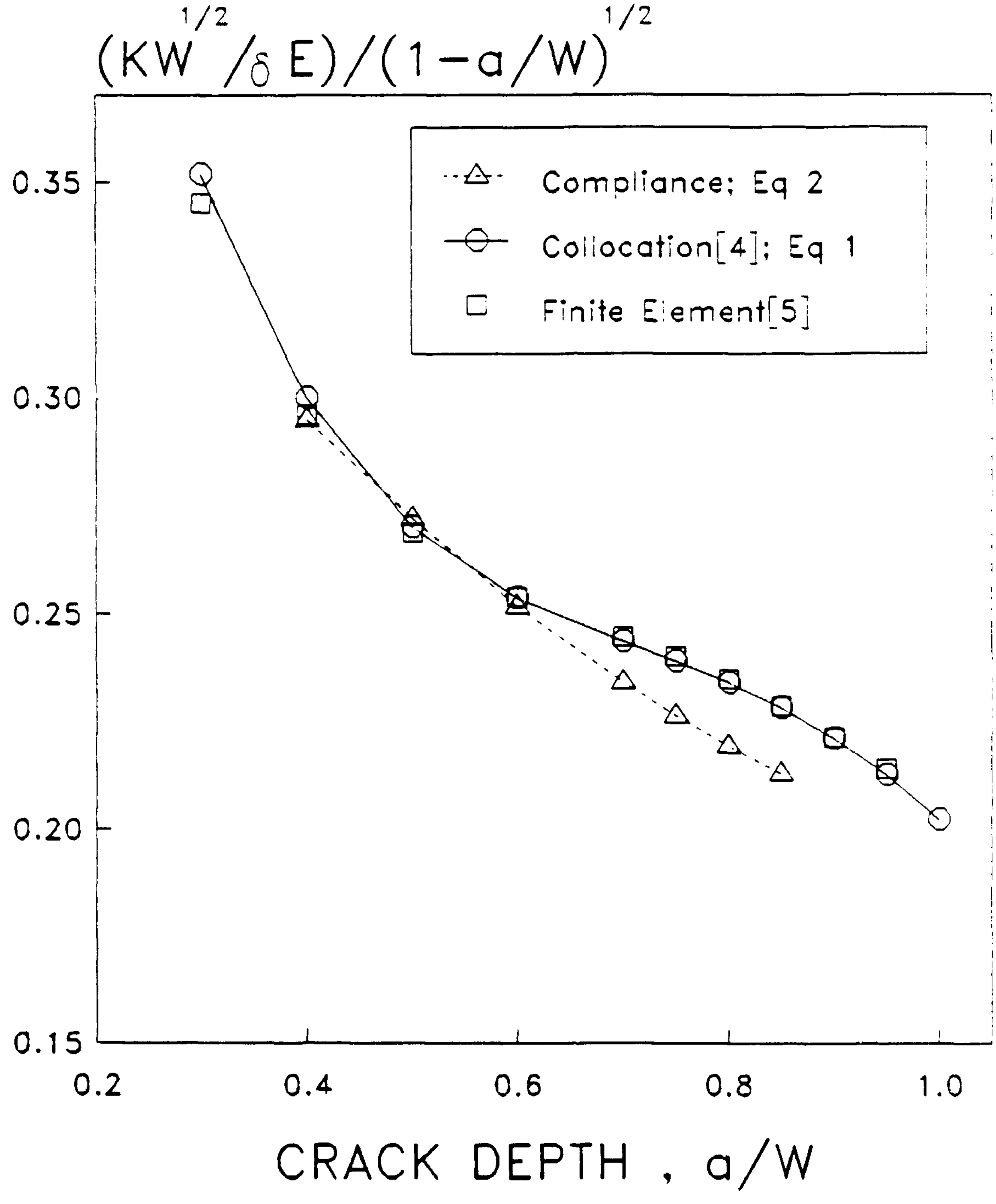

Figure 3. Comparison of K/δ results for wedge-loaded compact specimen.

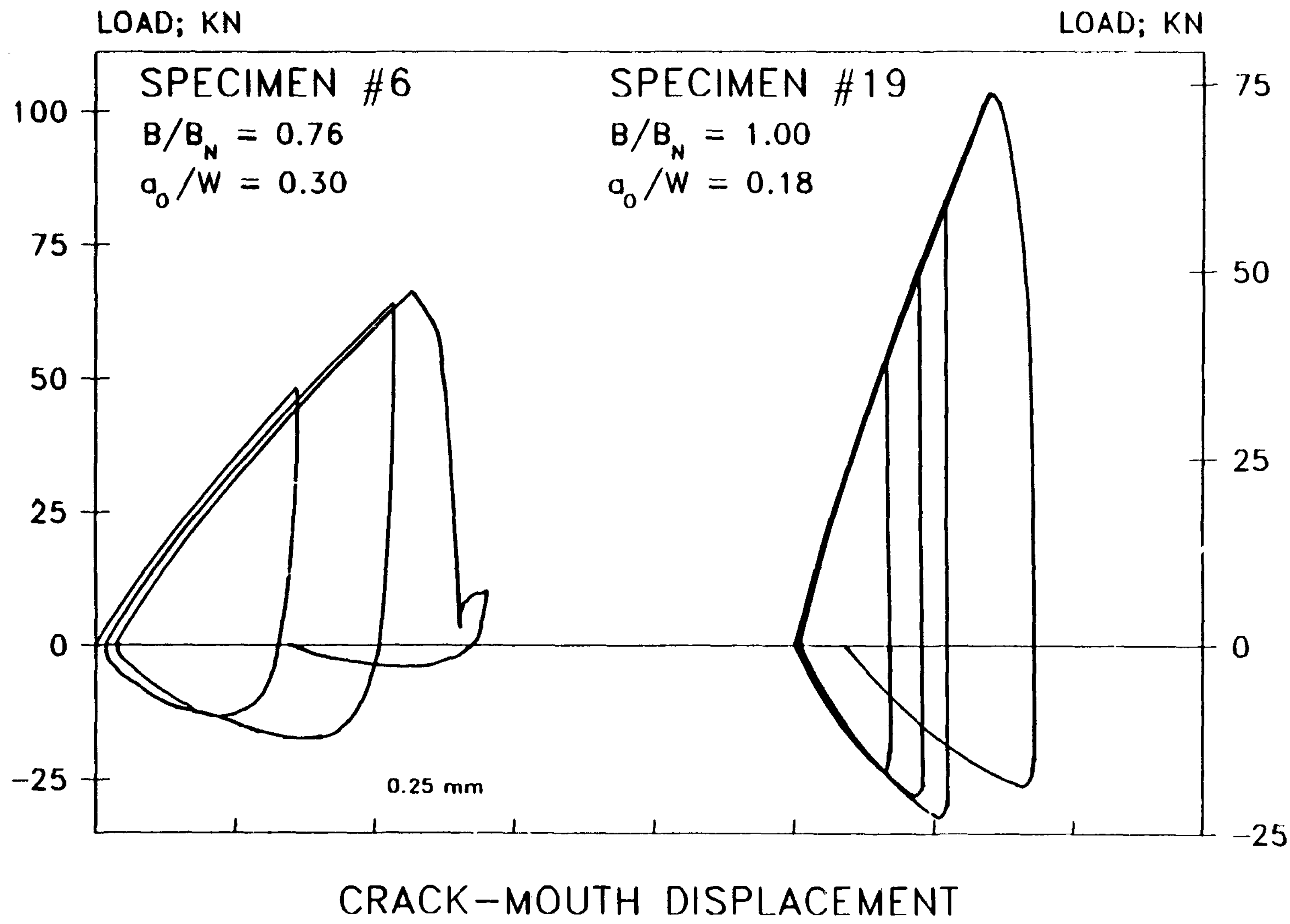

Figure 4. Wedge load versus crack-mouth displacement for K_{Ia} tests of BIS 690 at -60°C.

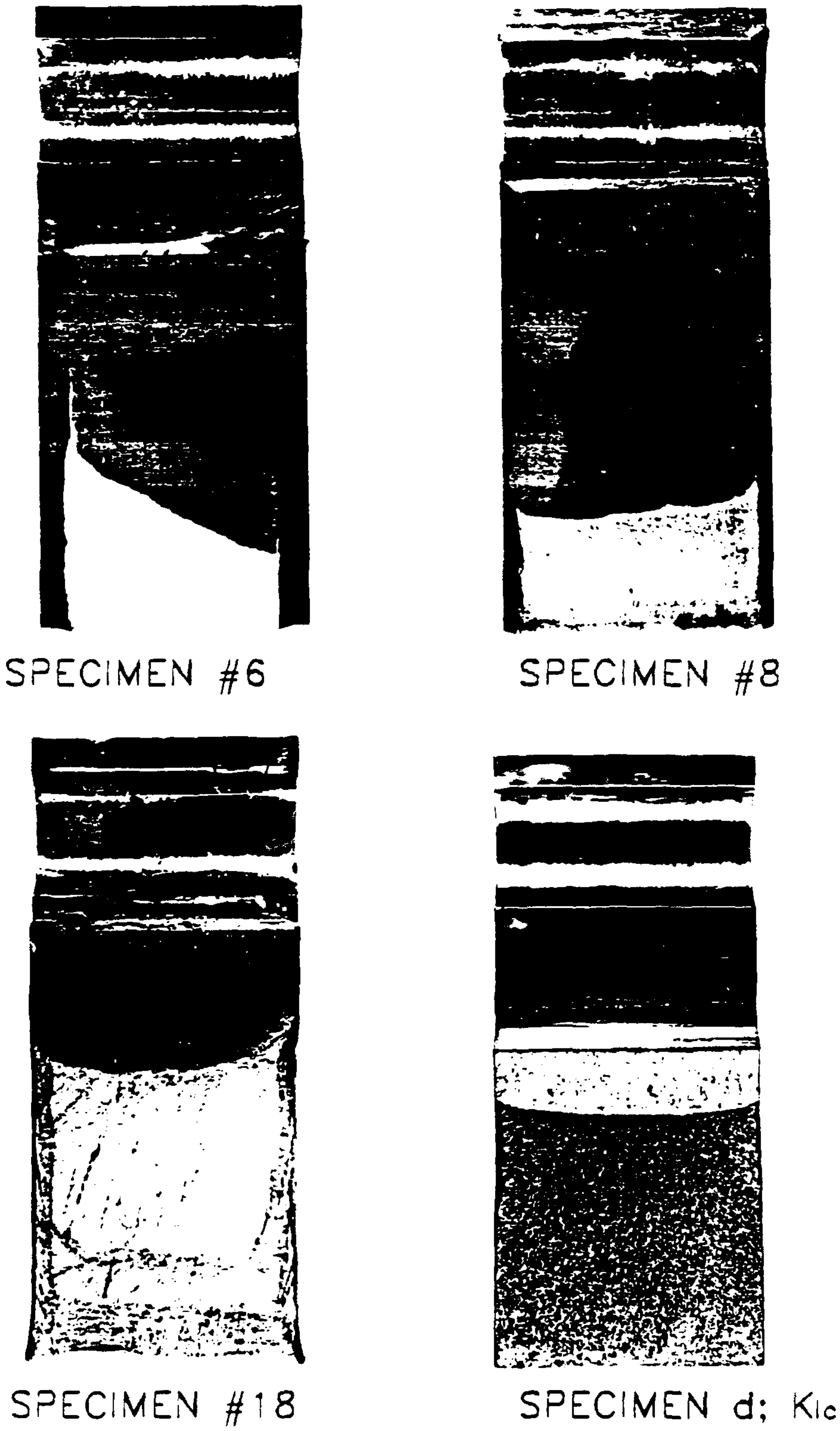

Figure 5. Photographs of fracture surfaces of K_{Ia} and K_{Ic} specimens.

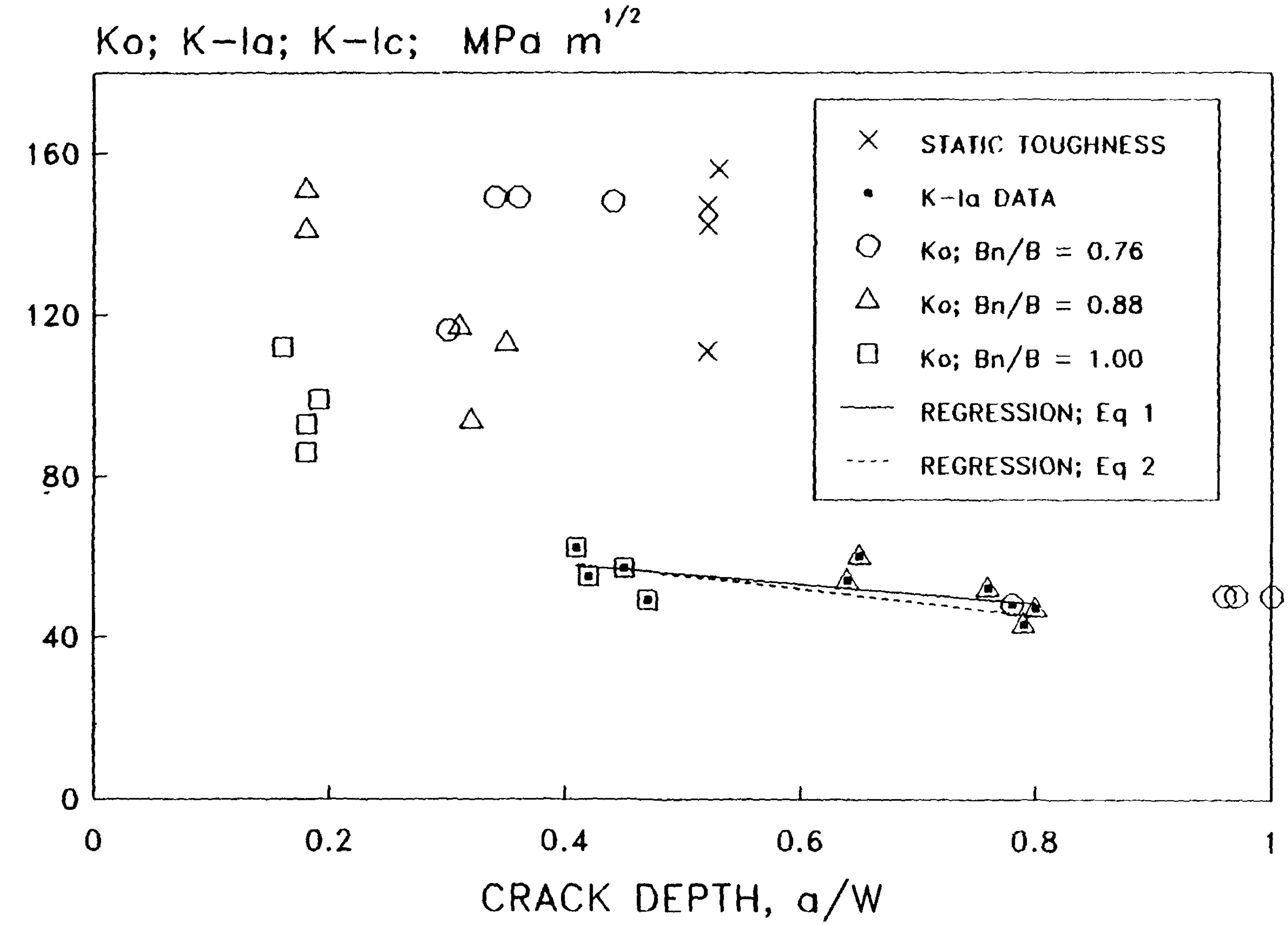

Figure 6. K_o, K_{Ic}, and K_{Ia} versus notch or crack depth.

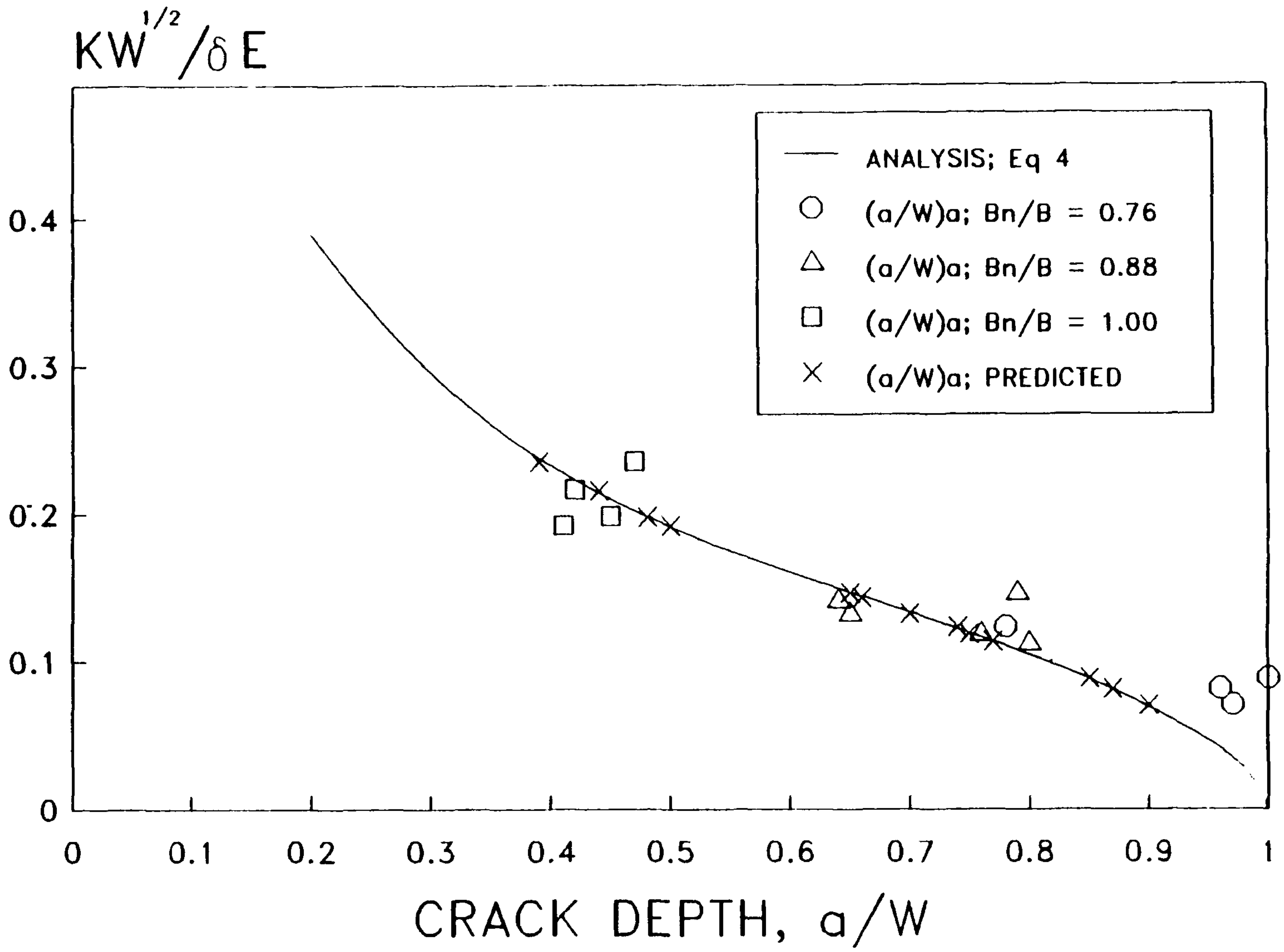

Figure 7. Calculated and measured values of $KW^{1/2}/\delta E$ versus crack depth.

TECHNICAL REPORT INTERNAL DISTRIBUTION LIST

	NO. OF COPIES
CHIEF, DEVELOPMENT ENGINEERING DIVISION	
ATTN: SMCAR-CCB-DA	1
-DC	1
-DI	1
-DR	1
-DS (SYSTEMS)	1
CHIEF, ENGINEERING SUPPORT DIVISION	
ATTN: SMCAR-CCB-S	1
-SD	1
-SE	1
CHIEF, RESEARCH DIVISION	
ATTN: SMCAR-CCB-R	2
-RA	1
-RE	1
-RM	1
-RP	1
-RT	1
TECHNICAL LIBRARY	5
ATTN: SMCAR-CCB-TL	
TECHNICAL PUBLICATIONS & EDITING SECTION	3
ATTN: SMCAR-CCB-TL	
OPERATIONS DIRECTORATE	1
ATTN: SMCWV-ODP-P	
DIRECTOR, PROCUREMENT DIRECTORATE	1
ATTN: SMCWV-PP	
DIRECTOR, PRODUCT ASSURANCE DIRECTORATE	1
ATTN: SMCWV-QA	

NOTE: PLEASE NOTIFY DIRECTOR, BENET LABORATORIES, ATTN: SMCAR-CCB-TL, OF ANY ADDRESS CHANGES.

TECHNICAL REPORT EXTERNAL DISTRIBUTION LIST

	NO. OF COPIES
ASST SEC OF THE ARMY RESEARCH AND DEVELOPMENT ATTN: DEPT FOR SCI AND TECH THE PENTAGON WASHINGTON, D.C. 20310-0103	1
ADMINISTRATOR DEFENSE TECHNICAL INFO CENTER ATTN: DTIC-FDAC CAMERON STATION ALEXANDRIA, VA 22304-6145	12
COMMANDER US ARMY ARDEC ATTN: SMCAR-AEE	1
SMCAR-AES, BLDG. 321	1
SMCAR-AET-O, BLDG. 351N	1
SMCAR-CC	1
SMCAR-CCP-A	1
SMCAR-FSA	1
SMCAR-FSM-E	1
SMCAR-FSS-D, BLDG. 94	1
SMCAR-IMI-I (STINFO) BLDG. 59 PICATINNY ARSENAL, NJ 07806-5000	2
DIRECTOR US ARMY BALLISTIC RESEARCH LABORATORY ATTN: SLCBR-DD-T, BLDG. 305 ABERDEEN PROVING GROUND, MD 21005-5066	1
DIRECTOR US ARMY MATERIEL SYSTEMS ANALYSIS ACTV ATTN: AMXSY-MP ABERDEEN PROVING GROUND, MD 21005-5071	1
COMMANDER HQ, AMCCOM ATTN: AMSMC-IMP-L ROCK ISLAND, IL 61299-6000	1

	NO. OF COPIES
COMMANDER ROCK ISLAND ARSENAL ATTN: SMCRI-ENM ROCK ISLAND, IL 61299-5000	1
DIRECTOR US ARMY INDUSTRIAL BASE ENGR ACTV ATTN: AMXIB-P ROCK ISLAND, IL 61299-7260	1
COMMANDER US ARMY TANK-AUTMV R&D COMMAND ATTN: AMSTA-DDL (TECH LIB) WARREN, MI 48397-5000	1
COMMANDER US MILITARY ACADEMY ATTN: DEPARTMENT OF MECHANICS WEST POINT, NY 10996-1792	1
US ARMY MISSILE COMMAND REDSTONE SCIENTIFIC INFO CTR ATTN: DOCUMENTS SECT, BLDG. 4484 REDSTONE ARSENAL, AL 35898-5241	2
COMMANDER US ARMY FGN SCIENCE AND TECH CTR ATTN: DRXST-SD 220 7TH STREET, N.E. CHARLOTTESVILLE, VA 22901	1
COMMANDER US ARMY LABCOM MATERIALS TECHNOLOGY LAB ATTN: SLCMT-IML (TECH LIB) WATERTOWN, MA 02172-0001	2

NOTE: PLEASE NOTIFY COMMANDER, ARMAMENT RESEARCH, DEVELOPMENT, AND ENGINEERING CENTER, US ARMY AMCCOM, ATTN: BENET LABORATORIES, SMCAR-CCB-TL, WATERVLIET, NY 12189-4050, OF ANY ADDRESS CHANGES.

TECHNICAL REPORT EXTERNAL DISTRIBUTION LIST (CONT'D)

	NO. OF COPIES
COMMANDER US ARMY LABCOM, ISA ATTN: SLCIS-IM-TL 2800 POWDER MILL ROAD ADELPHI, MD 20783-1145	1
COMMANDER US ARMY RESEARCH OFFICE ATTN: CHIEF, IPO P.O. BOX 12211 RESEARCH TRIANGLE PARK, NC 27709-2211	1
DIRECTOR US NAVAL RESEARCH LAB ATTN: MATERIALS SCI & TECH DIVISION	1
CODE 26-27 (DOC LIB) WASHINGTON, D.C. 20375	1
DIRECTOR US ARMY BALLISTIC RESEARCH LABORATORY ATTN: SLCBR-IB-M (DR. BRUCE BURNS) ABERDEEN PROVING GROUND, MD 21005-5066	1
COMMANDER AIR FORCE ARMAMENT LABORATORY ATTN: AFATL/MN EGLIN AFB, FL 32542-5434	1
COMMANDER AIR FORCE ARMAMENT LABORATORY ATTN: AFATL/MNF EGLIN AFB, FL 32542-5434	1
MIAC/CINDAS PURDUE UNIVERSITY 2595 YEAGER ROAD WEST LAFAYETTE, IN 47905	1

NOTE: PLEASE NOTIFY COMMANDER, ARMAMENT RESEARCH, DEVELOPMENT, AND ENGINEERING CENTER, US ARMY AMCCOM, ATTN: BENET LABORATORIES, SMCAR-CCB-TL, WATERVLIET, NY 12189-4050, OF ANY ADDRESS CHANGES.